INTERNATIONAL JOURNAL OF CONSERVATION SCIENCE

ISSN: 2067-533X Volume 16, Issue 2, 2025: 1013-1034 www.ijcs.ro

DOI: 10. 36868/IJCS.2025.02.17

MODELING OF HYDROLOGICAL AND MECHANICAL EFFECT OF VEGETATION ON LANDSLIDE

Yulia Amirul FATA[1,2,*], HENDRAYANTO[2,*], ERIZAL[3], Suria Darma TARIGAN[4]

[1] Department of Soil Science, Brawijaya University, Malang, Indonesia, 65145
[2] Department of Forest Management, IPB University, Bogor, Indonesia, 16680
[3] Department of Civil and Environmental Engineering, IPB University, Bogor, Indonesia, 16680
[4] Department of Soil and Land Resources Science, IPB University, Bogor, Indonesia, 16680

Abstract

Vegetation on a slope affects slope stability and landslides through the hydro-mechanical role of vegetation. This study aims to build a vegetation-slope stability model that describes the hydro-mechanical role of vegetation on slope stability and landslides. The novelty of this research is the slope stability model, namely the modified Simplified Bishop Method (SBM) using vegetation hydro-mechanical parameters. Soil hydro-mechanical parameters integrated into the modified SBM model are matrix suction (u_a–u_w), vegetation surcharges (S_w), wind load force (F_{wind}), root cohesion (C_R), and an interception, evapotranspiration in modifying soil water content (χ). The modeling results on eight scenarios of simulated slopes without vegetation and with vegetation of Teak (Tectona grandis), old Maesopsis eminii, young Maesopsis eminii, and shrubs (Chromolaena odorata) show an increase in FOS values such as 20.2%, 36.6%, 22.3%, and 7.3%, respectively. The FOS value increases with the shallower location of the phreatic line (PWP+), and the FOS value reaches stability (FOS > 1) when the PWP+ is ≥4 m deep except in old Maesopsis eminii with minimum soil mechanics parameters. However, old Maesopsis eminii reduces FOS by up to 2% when PWP+ ≥4 m because it has the largest S_w and F_{wind} and the smallest C_R among other vegetation. This study shows that the hydro-mechanical role of vegetation can increase slope stability compared to slopes without vegetation.

Keywords: *Hydrological; Mechanical; Vegetation; Slope stability; andslide*

Introduction

Landslides are the mass movement of soil, rock, rubble, or debris by gravity on a slope with the landslide movement types of rotational, translational, creep, flow, collapse, or combinations. Landslides are the third largest disaster in Indonesia after floods and tornadoes. There were more than 9500 landslides from 1815 to early 2024 in Indonesia, which caused more than 350 thousand fatalities and thousands of damages to facilities and infrastructure [1].

Static and dynamic factors cause landslides. Static factors include soil type, geology, slope steepness, and geomorphology [2]. Meanwhile, dynamic factors are divided into natural triggers (rainfall, earthquake) and human triggers (slope modification, land use changes, development activities, and mining) [3, 4]. The various factors that cause landslides require a detailed investigation of how landslides occur, especially on vegetated slopes. Investigating the process of landslides on vegetated slopes due to low slope stability is important, considering the

* Corresponding authors: yuliaafata@ub.ac.id and hendrayanto@apps.ipb.ac.id

dangers, casualties, and losses experienced, as well as the possibility for ecological restoration [5].

Vegetation strengthens the soil through mechanical and hydrological roles, influencing soil shear strength and slope stability. The hydrological vegetation role in slope stability models consists of matrix suction (u_a–u_w), water content (χ), root water uptake, and reducing soil moisture through evapotranspiration and interception [6, 7]. Meanwhile, the mechanical vegetation role in slope stability models consists of vegetation surcharges (S_w), wind load forces (F_{wind}), and root cohesion (C_R) [8, 9, 10, 11, 12].

The slope stability model consists of the Limit Equilibrium Method (LEM), Finite Element Method (FEM), and Spectral Element Method (SEM) to obtain the factor of safety (*FOS*) [13]. *FOS* is the ratio of shear resistance to shear stress. LEM is a method based on moment and force balance, assuming a circular or non-circular landslide. FEM models the stress-strain behavior of materials based on deformation, while SEM combines FEM with spectral-based model elements [14, 15].

Numerical modeling of the hydro-mechanical role of vegetation (u_a–u_w, χ, S_w, F_{wind}, C_R) in slope stability models has been widely used in several countries. In Kheyrud Forest, Iran uses a modified Bishop's LEM model with hydrological parameters (u_a–u_w, χ) and mechanical parameters (S_w, C_R) [3]; Hong Kong uses a modified slope stability model with hydrological parameters (u_a–u_w, χ) and mechanical parameters (C_R) [16]; Canada uses a modified FEM model with vegetation mechanical parameters (S_w, C_R) [17]; and Italy uses a modified slope stability model with vegetation hydrological parameters (u_a–u_w, χ) and vegetation mechanical parameters (C_R) [1].

Several studies have reviewed the hydro-mechanical role of vegetation on slope stability [9, 18], but not many studies have combined the five hydro-mechanical parameters of vegetation (u_a–u_w, χ, S_w, F_{wind}, C_R) in modeling slope stability. The vegetation types of *Maesopsis eminii*, teak (*Tectona grandis*), and shrubs (*Chromolaena odorata*) located on hillslopes that experience landslides were modeled. This study presents an analysis of the hydromechanical vegetation role on slope stability as an explanation of landslide mechanisms and their process on vegetated slopes.

Experimental part

Study Site

The research was conducted in the highlands of Mount Salak, which experienced a landslide on January 1, 2020. Pasir Madang Village, West Java Province. Geographically, Pasir Madang Village is located between 6°32'38.4" and 6°44'2.4" South Latitude and 106°25'1.2" to 106°31'19.2" East Longitude. The landslide that occurred was shallow and had circular and multiple rotational types. Landslide depth is between 1.5 and 10 meters. The area of the research site is 4.53ha.

The highlands of Mount Salak dominate the topography with elevations of more than 200 to 1920 masl. Moreover, the study site is between 675 and 740 masl. The slope steepness is dominated by 8-15%.

Land use consists of natural forests, mixed forests, plantation forests, industry, mixed plantations, fields, open land, settlements, paddy fields, oil palm plantations, and shrubs. The research plot was in a plantation forest consisting of teak (*Tectona grandis*), *Maesopsis eminii*, and shrubs (*Chromolaena odorata*).

The climate is Af-type according to the Köppen-Geiger classification. The Af climate is a tropical rainforest climate with a monthly rainfall of not less than 60mm/month [19]. The average monthly rainfall for ten years (2013-2022) is 163-328mm/month, with an average temperature of 22.3°C, wind speed of 71%, solar radiation of 73%, and air humidity of 3.6% [20]. Annual rainfall over the last ten years (2013-2022) ranges from 1953mm/year to 3938 mm/year, with a maximum rainy day of 21 days. Maximum monthly rainfall occurs in December-April.

The study site is in the Quaternary and Neogene geological periods with 11 geological formations. Meanwhile, the landslide was located on Endut volcanic rock (Qpv), consisting of breccia, lava, and volcanic tuff, and Quaternary volcanic rock (Qv) [21].

The Inceptisols soil type dominates the Sukajaya District, followed by the Andisol and Entisol soil types. Inceptisol is a developed soil with the suborders Aquepts and Udepts [22]. The depth of the Inceptisol soil solum is medium (51-75cm) to deep (76-100cm). The soil texture of Inceptisol is fine (clay variety) with slightly hampered drainage [23].

The research location is presented in figure 1, while the hydro-mechanical modeling stages of landslides are shown in figure 2.

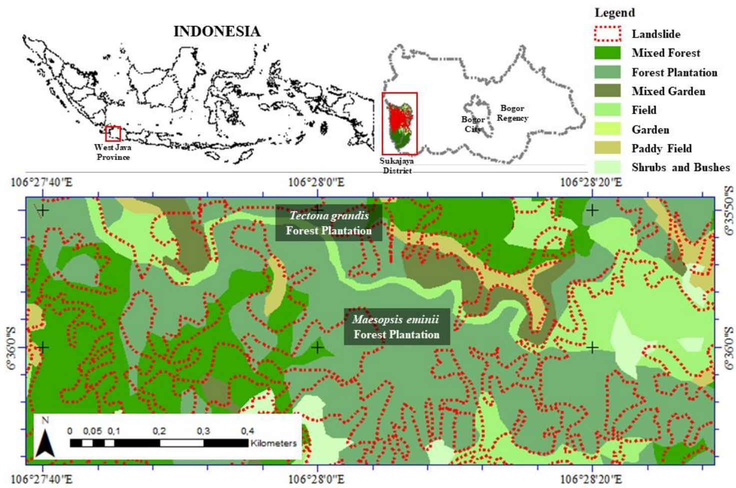

Fig. 1. Study Site

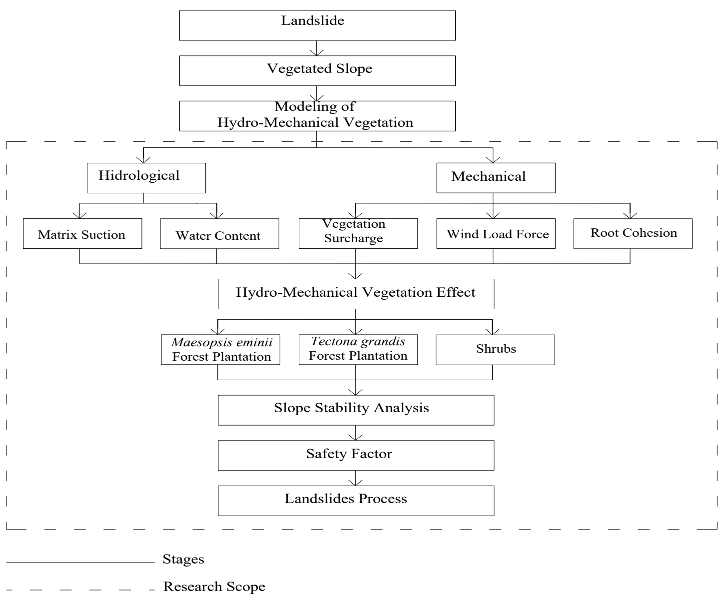

Fig. 2. Flow diagram of hydro-mechanical modeling of vegetation

Soil Parameter

Soil samples were collected from landslides and non-landslide slopes on the top, middle, and foot. Each sample location point is obtained at two depths, 0-50cm (Depth I) and 51-100cm (Depth II), with six sample location points on slopes without landslides and three on slopes with landslides. The diameter of the sample ring is 8cm, and the height of the sample ring is 40cm (Fig. 3).

Fig. 3. (A) Soil sampling on non-landslide; (B) Soil sampling on landslide; and (C) Hand drill set

Undisturbed soil samples are tested for soil shear strength using a direct shear test. Direct shear testing refers to [24] and [25]. The test objects were soil samples with three repetitions. The normal loads used are 0.5, 1, 1.5 and 2kgf. A direct shear test generated a graph showing the relation between normal stress and maximum shear stress. The regression equation is obtained from the relationship graph between maximum shear stress and normal stress to determine the value of effective soil cohesion (c') and effective internal friction angle (ϕ'). The mechanical soil parameters are presented in Table 1.

Table 1. Recapitulation of soil mechanical parameters for slope stability analysis [6]

Soil Mechanical Parameter		Depth I			Depth II		
		Min.	Average	Max.	Min.	Average	Max.
c'	(kPa)	1.68	3.06	4.87	1.08	2.53	4.87
ϕ'	(◦)	24.42	51.39	61.08	24.42	53.35	61.08
γ_{sat}	(kN/m3)	14.01	14.84	15.63	14.41	15.35	15.93

Slope Geometry Parameter

Slope stability modeling uses the slope profile obtained from geophysical studies with the Electrical Resistivity Tomography (ERT) technique. Previous research has been done in the 2D and 3D ground models at the preliminary stage by [9]. A slope profile was selected based on the 2D and 3D ground models, located 10 m below the surface. The profile can show two soil depth layers and consist of a low resistivity layer that represents a water-saturated layer as the seepage water table [6]. The seepage water table represents pore water pressure (PWP) layers in the slope.

Hydrological Vegetation Parameter

Hydrological vegetation parameters of matrix suction (ua–uw) and volumetric soil water content (χ) are modeled using pore water pressure (PWP) fluctuations as phreatic line input in slope stability modeling using Geostudio-Slope/W.

The PWP is described as a phreatic line representing the groundwater level presence in slope stability modeling. The groundwater level simulation scenario (phreatic line) is modeled every 1.0m depth on the slope profile (Fig. 4).

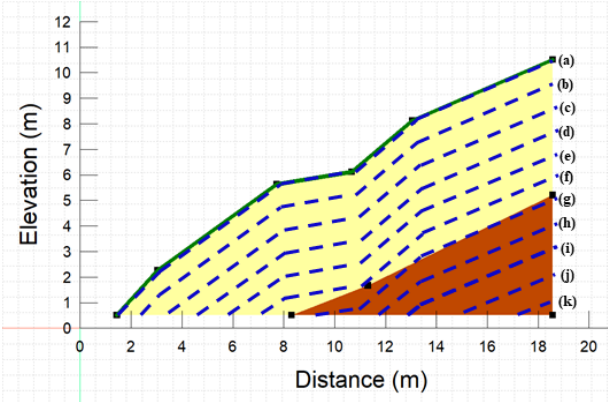

Fig. 4. Phreatic line simulation for modelling slope stability

Mechanical Vegetation Parameter

Mechanical Vegetation Parameter 1: Root Cohesion (CR)

Root sampling of old and young teak, Maesopsis eminii, and shrubs was carried out in January 2021 (Figure 5). Samples of vegetation roots were chosen to reflect three classes of root diameters: class I (>5–≤10mm), class II (≥2.5–≤5mm), and class III (<2.5mm). CR estimation only considers root diameters in the 1–10mm range. Root samples were air-dried after being soaked in water for approximately 14 days before root testing [4].

(I) (II) (III)

Fig. 5. Root sampling plots: (I) Teak; (II) old Maesopsis eminii; and (III) young Maesopsis eminii

Diameter classes I, II and III roots measuring 15cm in length were tested in two repetitions [26] to determine the root tensile strength testing speed, which is 5mm/s in diameter class I and 1.0mm/s in diameter classes II and III [6]. Root tensile strength (TR) was calculated using [27]. CR was calculated using [28], which is a function of TR and root area ratio (RAR).

The maximum CR is in diameter class I and the largest CR was in teak, followed by old Maesopsis eminii, young Maesopsis eminii, and shrubs at 0.284, 0.043, 0.177 and 0.154kPa, respectively. Summation of CR in each root diameter class in each vegetation used to obtain total CR. The largest total CR in teak was 0.398kPa, followed by shrubs and young and old Maesopsis eminii with total root cohesion values of 0.202, 0.191 and 0.087kPa, respectively. The greater the total CR, the larger the root contribution, which increases the soil shear strength. When the soil has high root biomass or matches each vegetation's root depth, the soil's shear strength increases [6]. Total CR and root depth are used as parameters in slope stability analysis.

Mechanical Vegetation Parameter 2: Vegetation Surcharges (Sw)

Sw of Teak and Maesopsis eminii is obtained by estimating the above-ground biomass (AGB) (kg) of each tree based on equation (1) and the Sw is calculated based on equation (2).

$$AGB = \alpha(DBH)^{\beta} \quad (1)$$

$$S_w = \frac{1}{A_l}\sum_{i=1}^{n} AGB \times g \times (1+\omega) \quad (2)$$

Equation (1) shows the estimation of AGB based on tree diameter at breast height (DBH, m), α and β based on the results of the allometric AGB equation of studies related to the Tectona grandis obtained from research by [29] and Maesopsis eminii obtained from research by [30]. Vegetation surcharges (Sw, kPa), g is the gravity value (N/kg), ω is the tree water content (without dimensions), n is the number of trees, and Al is the area of the slope (m2). ω of Tectona grandis was 70.79% [31], while ω of Maesopsis eminii was 112.78% [32]. Sw of Chromolaena odorata was obtained by [33]. The estimated vegetation surcharges based on Equation 2 are presented in Table 2.

Table 2. Recapitulation of Sw

Plot	Vegetation	Sample	A (m2)	AGB (kg/tree)	g (N/kg)	ω	Sw (N/m2)	Sw (kPa)	Average Sw (kPa)
1	Teak	a	1.888	13.656	9.8	0.7079	121.084	0.121	0.209
		b	5.069	60.272	9.8	0.7079	199.010	0.199	
		c	11.346	208.414	9.8	0.7079	307.457	0.307	
2	Young Maesopsi eminii	a	3.768	1.290	9.8	1.1278	7.137	0.007	0.029
		b	1.607	1.848	9.8	1.1278	23.984	0.024	
		c	5.728	15.541	9.8	1.1278	56.576	0.057	
3	Old Maesopsi eminii	a	13.728	14.449	9.8	1.1278	21.947	0.022	0.133
		b	2.807	46.212	9.8	1.1278	343.337	0.343	
		c	5.813	48.393	9.8	1.1278	173.593	0.174	
		d	4.755	8.870	9.8	1.1278	38.900	0039	
		e	13.926	57.730	9.8	1.1278	86.443	0.086	
4	Shrubs	a	1.000	0.935	9.8	0.704	15.614	0.016	0.016
		b	1.000	0.935	9.8	0.704	15.614	0.016	
		c	1.000	0.935	9.8	0.704	15.614	0.016	
		d	1.000	0.935	9.8	0.704	15.614	0.016	

Table 2 shows that the Sw value in teak ranges from 0.121 to 0.121–0.307kPa, in young Maesopsis eminii ranges from 0.007 to 0.057kPa, in old Maesopsis eminii ranges from 0.022–0.343kPa, and in shrubs is 0.016kPa. The average Sw on teak, young and old Maesopsis eminii, and shrubs is 0.209, 0.029, 0.133, and 0.016kPa, respectively. Sw increases normal stress, which improves soil resistance to movement [34] and reduces the possibility of soil movement downslope [28]. Meanwhile, Sw provides slope pressure (destabilization) [35] and increases the mass that has the potential to cause landslides [3, 36].

Mechanical Vegetation Parameter 3: Wind Load Forces (Fwind)

Fwind on trees is transmitted as moments and forces through the branches down to the ground by the root system [37]. Fwind tends to reduce slope stability [35]. Y. Kim, et al. [37] state the equation for Fwind as follows (Equation 3).

$$F_{wind} = \frac{1}{2}\rho_{air} {v_a}^2 C_D A_t \quad (3)$$

where: Fwind is the wind load force (N), ρ air is the air density (kg/m3), va is the wind speed (m/sec), CD is the drag coefficient [38], and At is the area of the trunk and crown of vegetation exposed to the wind (m2).

Vegetation characteristics and Fwind parameters in teak and Maesopsis eminii are presented in Table 3. Fwind on the shrubs was neglected in this study.

Table 3. Wind load force parameters and vegetation characteristics

Plot	Vegetation	Sample	Height (m)	Crown Diameter (m)	ρ (kg/m3)	va (m/s)	CD	At (m2)	Fwind (N)
1	Tectona grandis	a	6.5	1.55	1.2	12	1.24	1.89	202.24
		b	11.5	2.54	1.2	12	1.24	5.07	543.08
		c	11.5	3.80	1.2	12	1.24	11.35	1215.53
		d	11.0	2.75	1.2	12	1.24	5.94	636.60
		e	14.0	3.79	1.2	12	1.24	11.29	1209.15
2	Maesopsis eminii	a	3.0	2.19	1.2	12	1.04	3.77	338.61
		b	4.0	1.43	1.2	12	1.04	1.61	144.37
		c	5.5	2.70	1.2	12	1.04	5.73	514.68
3	Maesopsis eminii	a	12.5	5.87	1.2	12	1.17	27.07	2736.78
		b	11.0	2.22	1.2	12	1.17	3.85	389.68
		c	6.5	4.18	1.2	12	1.17	13.73	1387.77
		d	8.5	1.89	1.2	12	1.17	2.81	283.72
		e	11.5	2.72	1.2	12	1.17	5.81	587.63
		f	9.5	2.46	1.2	12	1.17	4.75	480.66
		g	10.5	4.21	1.2	12	1.17	13.93	1407.76

The maximum Fwind in the teak, young and old Maesopsis eminii is 1215.53 N, 514.68 N, and 2736.78 N. The lowest Fwind is in the young Maesopsis eminii, and the highest is in the old Maesopsis eminii. [39] explained that varying plant age significantly influences mechanical properties because the modulus of elasticity varies between species and plant age. Fwind, as one of the mechanical properties of vegetation, does not scale linearly with tree size [40]. Moreover, the maximum value is used to model slope stability.

Slope Stability Modeling Using GeoStudio-SLOPE/W

The factor of safety (FOS) is determined by modeling the slope stability using the limit equilibrium method (LEM) [41]. Slope stability is presented based on the FOS value, with the general Mohr-Coulomb equation shown in equation 4.

$$FOS = \frac{\tau}{\tau_d} \tag{4}$$

where: FOS is the factor of safety, τ is the maximum shear strength available in the soil, and τd is the shear stress that occurs due to the soil gravity. The soil shear strength is based on the Coulomb equation [42] shown in Equation 5.

$$\tau = c' + \sigma_n \tan \phi' \tag{5}$$

where: c' is the effective soil cohesion, σn is the normal stress, and ϕ' is the effective friction angle. The above equation was developed by including the PWP parameter [34, 43, 44], shown in equation (6), used in saturated soils.

$$\tau = c' + [\sigma_n - u_w] \tan \varphi' \tag{6}$$

where: uw is the pore water pressure.

Soil shear strength can be defined as effective stress. Effective stress equals the degree of effective water saturation [45]. R.H. Brooks and A.T. Corey [46] describe the parameters as follows.

$$\chi = \left(\frac{S-S_r}{1-S_r}\right)^{0,55/\lambda} \quad (7)$$

where: S is the degree of saturation, Sr is the degree of residual saturation, and λ is the pore size distribution index. Sr represents the greatest saturation at which capillary absorption forces retain pore water. S is a function of the maximum shear stress in unsaturated soil based on the soil water characteristic curve (SWCC) [47]. Shear strength in unsaturated soil is a function of volumetric water content (Θ) and matrix suction (ua–uw) [8], which is shown in equation 8.

$$\tau = c' + (\sigma_n - u_a)\tan\varphi' + (u_a - u_w)\left[\left(\frac{\theta-\theta_r}{\theta_s-\theta_r}\right)\tan\varphi'\right] \quad (8)$$

The slice method is one of the LEM models that is applied to inhomogeneous soils with unpredictable seepage fluxes. Bishop developed the Simplified Bishop Method (SBM) by calculating the forces around the slice plane with FOS values close to field conditions [48] and close to models based on moment and force balance [14]. The circular slip surface, acting forces, and vegetation parameters on slope stability in the Bishop model are presented in Figure 6.

The normal force at a point on the landslide plane circle (O) with a specific circle radius (R) is influenced by the weight of the soil (Wsoil). The SBM divides the landslide mass into several vertical slices. The forces consist of shear force (Xi and Xi+1) and effective normal force (Ei and Ei+1) along the slice. The resultant effective shear force (Ti) and the resultant effective normal force (Ni) work along the bottom of the wedge. Pore water pressure (ui and ui+1) works on both wedges, and pore water pressure (Ui) performs at the bottom of the wedge. The soil slice also has the soil slice angle (θi) and the soil slice width (bi). Moreover, there are also original soil parameters and soil parameters influenced by vegetation. Vegetation parameters also affect the normal load acting on the ground (Fig. 6).

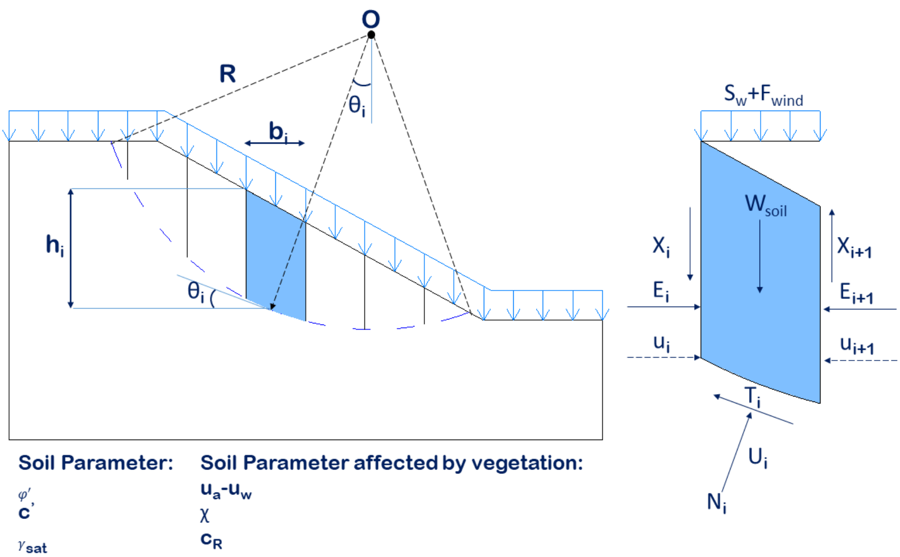

Fig. 6. Circular shear field, acting forces, and vegetation parameters on SBM slope stability (modification from [12] and [26])

The factor of safety (FOS) of the Simplified Bishop Method (SBM) is presented in equation (10).

$$FOS = \frac{\sum_{i=1}^{n}\left[\frac{(c'b_i)+(W_i-u_{wi}b_i)tg\phi}{ma}\right]_i}{\sum_{i=1}^{n} W_i \sin\theta_i} \tag{10}$$

$$(ma)_i = \cos\theta_i + \frac{\sin\theta_i \tan\phi'_i}{FOS} \tag{11}$$

where: Wi is the soil weight of slice-i (kN), c' is the effective soil cohesion (kN/m2), φ′ is the effective angle friction in the soil (°), θi is the angle of the soil slice (o), uw is the pore water pressure (kN/m²), and b is the slice width (m).

Substitution of the vegetation role on slope stability by matrix suction (ua–uw), volumetric soil water content (χ), vegetation surcharges (Sw), wind load force (Fwind), and root cohesion (CR) in the SBM model, forming a new FOS equation (12), which is a modification of [12], who previously used an SBM that consisted of four vegetation roles (ua–uw, χ, Sw, and CR). Five hydro-mechanical vegetation parameters modified the SBM and were then classified as the finite element method (FEM).

Equation (12) is an SBM modified with the hydro-mechanical vegetation in saturated soil, while equation (13) is in unsaturated soil.

$$FOS = \frac{\sum_{i=1}^{n}\left[\frac{(c'+c'_R)b_i+(W_i-u_{wi}b_i+S_w b_i)tg\phi'+(u_a-u_w)b_i tg\phi}{ma}\right]_i}{\sum_{i=1}^{n}(W_i+S_w b_i+F_{wind} b_i)\sin\theta_i} \tag{12}$$

$$FOS = \frac{\sum_{i=1}^{n}\left[\frac{(c\prime+c\prime_R)b_i+(W_i-u_{wi}b_i+S_w b_i)tg\phi\prime+(u_a-u_w)\left(\frac{\Theta_w-\Theta_r}{\Theta_s-\Theta_r}\right)b_i tg\phi\prime}{ma}\right]_i}{\sum_{i=1}^{n}(W_i+S_w b_i+F_{wind} b_i)\sin\theta_i} \tag{13}$$

Slope stability modeling analyzes various soil types, complex stratigraphy, slip surface planes, and PWP conditions. Slope stability analysis was carried out to model the hydro-mechanical role of vegetation and produce the factor of safety (FOS) value. Eight scenarios were compared with bareland (without vegetation), such as (A) teak, (B) old Maesopsis eminii, (C) young Maesopsis eminii, (D) shrubs (Chromolaena odorata), (Aa) teak with shrubs, (Bb) old Maesopsis eminii with shrubs, and (Cc) young Maesopsis eminii with shrubs (Fig. 7).

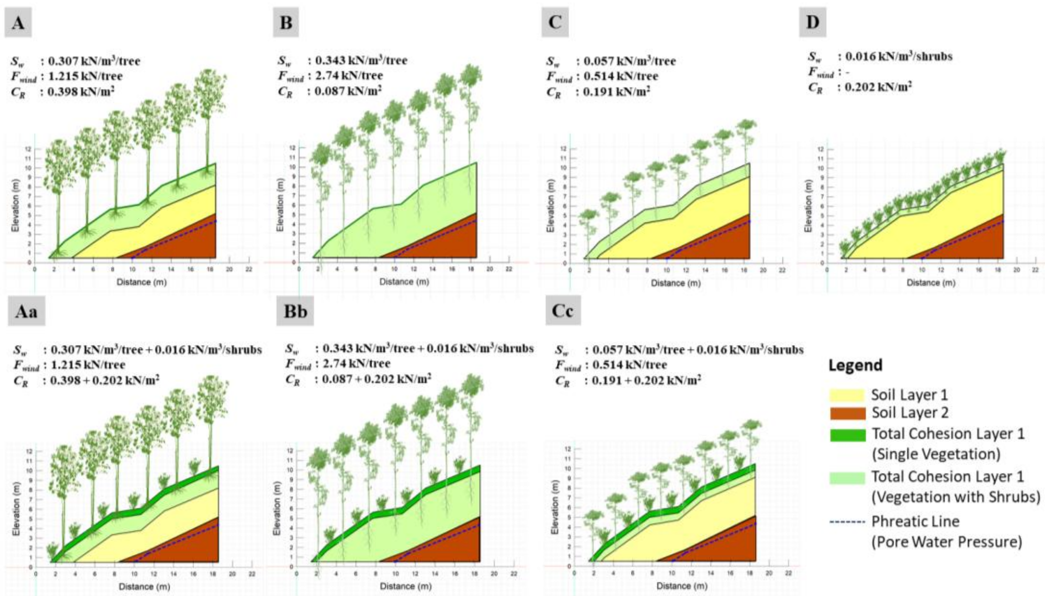

Fig. 7. Slope geometric profiles influenced by the effective depth of root cohesion in teak, young and old Maesopsis eminii, and shrubs (Chromolaena odorata) vegetation

Verification of Hand Calculations for Slope Stability Modeling

Slope stability modeling requires verification based on calculations of FOS. Verification refers to the "Verification-Hand Calculations" that are formulated based on the limit equilibrium theory (LEM) guide from [41]. The verification process can validate the slope stability modeling.

The SBM considers interslice normal forces. The normal force (N) at the bottom of the slice is determined by the summation of forces in the vertical direction. Furthermore, N becomes an FOS function with the following equation:

$$N = \frac{W - \frac{(c'b\sin\theta - u_w b \sin\theta \tan\phi')}{FOS}}{\cos\theta + \frac{\sin\theta\tan\phi'}{FOS}} \tag{14}$$

The denominator in the equation (14) is a variable called ma. FOS SBM can then be calculated as follows:

$$FOS = \frac{\sum[c'b + (N - u_w b)\tan\phi']}{\sum W \sin\theta} \tag{15}$$

The normal force (N) in Equation 14 is a function of FOS, while FOS is also a function of N (Equation 15). Therefore, an iterative solution procedure in the SBM is needed to solve the equation. Equations 14 and 15 are then substituted using hydro-mechanical vegetation parameters (ua–uw, χ, Sw, Fwind, CR) and being new FOS equation (16) and equation (17).

$$N = \frac{W - \frac{\left((c' + c'_R)b\sin\alpha - u_w b\sin\theta\tan\phi'\right)}{FOS}}{\cos\theta + \frac{\sin\theta\tan\phi'}{FOS}} \tag{16}$$

$$FOS = \frac{\sum[c'b+(N-u_w b+S_w b)\tan\phi'+(u_a-u_w)b\tan\phi']}{\sum(W+S_w b+F_{wind}b)\sin\theta} \quad (17)$$

Results and discussion

Factor of Safety

The hydrological vegetation role (χ, ua–uw) is modeled through PWP at a depth of every 1 m. The mechanical role (CR, Sw, Fwind) is modeled by adding CR and effective soil cohesion (c') to the soil mechanics parameters, Sw as a surface surcharge, and Fwind as a point load in the ground surface. The simulation produces CR, Sw, and Fwind parameters, with the respective units being kPa, kN/m3, and kPa. The parameters are used as input for slope stability modeling based on the modified SBM-vegetation equation.

Finite Element Method (FEM) analysis of the modified SBM-vegetation model used to model the hydro-mechanical role of vegetation on slope stability. Slope stability modeling produces FOS values based on minimum, average, and maximum soil mechanical parameters, which are presented in Tables 4, 5 and 6, respectively.

Table 4. FOS recapitulation in 8 modeling scenarios at each PWP depth based on minimum soil mechanics parameters

Phreatic Line		FOSmin							
Code	Depth (m)	Bareland	A	Aa	B	Bb	C	Cc	D
a	0	0.247	0.297	0.297	0.332	0.334	0.3	0.302	0.265
b	1	0.546	0.569	0.567	0.595	0.596	0.602	0.613	0.576
c	2	0.767	0.845	0.847	0.855	0.857	0.872	0.894	0.858
d	3	0.951	1.01	1.009	0.988	0.995	1.054	1.064	1.034
e	4	1.01	1.026	1.029	0.988	0.995	1.061	1.064	1.041
f	5	1.01	1.026	1.029	0.988	0.995	1.061	1.064	1.041
g	6	1.01	1.026	1.029	0.988	0.995	1.061	1.064	1.041
h	7	1.01	1.026	1.029	0.988	0.995	1.061	1.064	1.041
i	8	1.01	1.026	1.029	0.988	0.995	1.061	1.064	1.041
j	9	1.01	1.026	1.029	0.988	0.995	1.061	1.064	1.041
k	10	1.01	1.026	1.029	0.988	0.995	1.061	1.064	1.041

Table 5. FOS recapitulation in 8 modeling scenarios at each PWP depth based on average soil mechanics parameters

Phreatic Line		FOSaverage							
Code	Depth (m)	Bareland	A	Aa	B	Bb	C	Cc	D
a	0	0.629	0.745	0.747	0.857	0.859	0.756	0.758	0.674
b	1	1.477	1.525	1.526	1.598	1.599	1.611	1.638	1.548
c	2	2.051	2.245	2.248	2.277	2.281	2.361	2.417	2.323
d	3	2.53	2.594	2.598	2.525	2.531	2.716	2.718	2.658
e	4	2.581	2.594	2.598	2.525	2.531	2.716	2.718	2.658
f	5	2.581	2.594	2.598	2.525	2.531	2.716	2.718	2.658
g	6	2.581	2.594	2.598	2.525	2.531	2.716	2.718	2.658
h	7	2.581	2.594	2.598	2.525	2.531	2.716	2.718	2.658
i	8	2.581	2.594	2.598	2.525	2.531	2.716	2.718	2.658
j	9	2.581	2.594	2.598	2.525	2.531	2.716	2.718	2.658
k	10	2.581	2.594	2.598	2.525	2.531	2.716	2.718	2.658

Table 6. FOS recapitulation in 8 modeling scenarios at each PWP depth based on maximum soil mechanics parameters

Phreatic Line		FOSmax							
Code	Depth (m)	Bareland	A	Aa	B	Bb	C	Cc	D
a	0	1.070	1.214	1.215	1.366	1.367	1.250	1.252	1.136
b	1	2.250	2.310	2.311	2.406	2.407	2.440	2.475	2.351
c	2	3.040	3.301	3.304	3.344	3.349	3.480	3.572	3.417
d	3	3.698	3.752	3.757	3.67	3.676	3.944	3.947	3.864
e	4	3.754	3.752	3.757	3.67	3.676	3.944	3.947	3.864
f	5	3.754	3.752	3.757	3.67	3.676	3.944	3.947	3.864
g	6	3.754	3.752	3.757	3.67	3.676	3.944	3.947	3.864
h	7	3.754	3.752	3.757	3.67	3.676	3.944	3.947	3.864
i	8	3.754	3.752	3.757	3.67	3.676	3.944	3.947	3.864
j	9	3.754	3.752	3.757	3.67	3.676	3.944	3.947	3.864
k	10	3.754	3.752	3.757	3.67	3.676	3.944	3.947	3.864

Note: Blue indicates FOS <1

The results of slope stability modeling show variations in FOS. Slopes with old Maesopsis eminii had the greatest FOS when PWP was at the ground surface, while when PWP was at a depth of >1m, the largest FOS was young Maesopsis eminii, followed by shrubs, teak, old Maesopsis eminii, and bareland.

The results of slope stability modeling in minimum soil mechanical parameters (Table 4) show that with a PWP of 0-2m, FOS <1 (unsafe). FOS <1 also occurs in the bareland scenario with a PWP of 3m and on old Maesopsis eminii (scenario B and scenario Bb). This is influenced by the largest Sw and Fwind, as well as the smallest CR (Figure 7). Sw and Fwind as a function of shear stress tend to reduce slope stability. Meanwhile, CR, the largest function of shear resistance in hydro-mechanical vegetation parameters, is also relatively low (0.087kPa). Slope stability in average soil mechanical parameters (Table 5), FOS <1 only occurs at the PWP on the soil surface, which indicates that all soil layers are saturated. Meanwhile, in the slope stability in maximum soil mechanical parameters (Table 6), FOS is >1 (safety).

FOS increases with increasing depth of PWP and begins to stabilize at a PWP of 4m on slopes without vegetation and at a PWP of 3m on slopes with vegetation. Furthermore, the groundwater level fluctuations affect FOS, and FOS is stable at a PWP depth of 3-4m and beyond. [49] and [50] show that extreme rainfall more affects shallow soil depth, and FOS decreases as rainfall intensity increases (infiltration is higher). The effective depth of vegetation is related to the maximum root depth, with teak, old Maesopsis eminii, young Maesopsis eminii, and shrubs having maximum root depths of 230, 500, 140, and 66cm, respectively.

The presence of vegetation can increase slope stability. Modeling results show that the highest FOS is in young Maesopsis eminii, followed by shrubs, teak, and old Maesopsis eminii. FOS of old Maesopsis eminii tends to be lower than bareland values (Tables 4 to 6). Moreover, FOS changes are presented in Figure 8.

The increase in FOS is different in each scenario of soil mechanical parameters. The largest FOS changes generally occur at minimum soil mechanical parameters, while the FOS changes are smaller at maximum soil mechanical parameters.

FOS increased in teak, young Maesopsis eminii, and shrubs. Meanwhile, FOS of old Maesopsis eminii increased at PWP 0-4m (scenarios a-d) and decreased when PWP>4m. The largest FOS increase is when PWP is at the ground surface (PWP=0m) in teak, old Maesopsis eminii, and young Maesopsis eminii, while FOS in shrubs increases when PWP is at a depth of 2m (scenario c).

Table 7. Calculation with trial $FOS = 0.758$ (shear strength/shear stress)

Slice	ϕ'	$\tan\phi'$	θ	ma	$c' + c'_R$	u_a	u_w	u_a-u_w	S_w	F_{wind}	W	b	N	*Shear strength*	*Shear stress*
	°	kPa	°	°	kPa	kPa	kPa	kN	kN	kN	kN	m			
1	51.39	1.25	46.83	2.17	3.457	0.00	2.1635	-2.16	0.00000	0	2.276	0.695	0.76	1.476	1.660
2	51.39	1.25	12.21	1.41	3.457	0.00	3.2434	-3.24	0.00037	0	0.308	0.063	0.23	0.247	0.065
3	51.39	1.25	12.56	1.42	3.457	0.00	4.7408	-4.74	0.00000	0	2.042	0.285	1.61	1.316	0.444
4	51.39	1.25	13.12	1.44	3.256	0.00	7.1793	-7.18	0.00000	0	3.097	0.285	2.58	1.591	0.703
5	51.39	1.25	13.44	1.45	3.256	0.00	8.5443	-8.54	0.00000	0	0.465	0.036	0.39	0.223	0.108
6	51.39	1.25	13.68	1.45	3.256	0.00	9.1607	-9.16	0.00000	0	2.759	0.199	2.33	1.284	0.652
7	51.39	1.25	13.99	1.46	3.256	0.00	9.8939	-9.89	0.00564	0.514	1.749	0.117	1.48	0.790	0.437
8	51.39	1.25	14.51	1.48	3.256	0.00	11.07	-11.07	0.00000	0	6.730	0.402	5.73	2.908	1.686
9	51.39	1.25	15.31	1.50	3.256	0.00	12.853	-12.85	0.00000	0	7.815	0.402	6.67	3.200	2.064
10	51.39	1.25	16.36	1.53	3.06	0.00	15.059	-15.06	0.00000	0	14.518	0.637	12.47	5.556	4.089
11	51.39	1.25	17.08	1.56	3.06	0.00	16.549	-16.55	0.00041	0	2.008	0.080	1.73	0.747	0.590
12	51.39	1.25	17.73	1.57	3.06	0.00	17.79	-17.79	0.00000	0	14.836	0.551	12.77	5.396	4.517
13	51.39	1.25	18.85	1.61	3.06	0.00	19.89	-19.89	0.00000	0	16.587	0.551	14.28	5.841	5.359
14	51.39	1.25	19.53	1.62	3.06	0.00	21.119	-21.12	0.00598	0.514	3.737	0.117	3.22	1.295	1.270
15	51.39	1.25	20.15	1.64	3.06	0.00	22.152	-22.15	0.00000	0	15.999	0.477	13.77	5.469	5.510
16	51.39	1.25	21.13	1.67	3.06	0.00	23.754	-23.75	0.00000	0	17.157	0.477	14.77	5.757	6.185
17	51.39	1.25	22.13	1.69	3.06	0.00	25.263	-25.26	0.00000	0	18.247	0.477	15.71	6.028	6.873
18	51.39	1.25	22.73	1.71	3.06	0.00	26.135	-26.14	0.00050	0	3.800	0.096	3.27	1.245	1.468
19	51.39	1.25	22.93	1.72	3.06	0.00	26.419	-26.42	0.00000	0	3.934	0.098	3.39	1.285	1.533
20	51.39	1.25	23.05	1.72	3.06	0.00	26.581	-26.58	0.00000	0	0.547	0.014	0.47	0.178	0.214
21	51.39	1.25	23.79	1.74	3.06	0.00	25.664	-25.66	0.00000	0	26.757	0.689	22.97	8.732	10.794
22	51.39	1.25	24.64	1.76	3.06	0.00	24.565	-24.57	0.00545	0.514	4.187	0.113	3.58	1.369	1.770
23	51.39	1.25	25.38	1.78	3.06	0.00	23.528	-23.53	0.00000	0	20.439	0.574	17.45	6.694	8.759
24	51.39	1.25	26.61	1.81	3.06	0.00	21.703	-21.70	0.00000	0	18.855	0.574	16.02	6.213	8.446
25	51.39	1.25	27.31	1.82	3.06	0.00	20.635	-20.64	0.00035	0	2.152	0.069	1.82	0.713	0.987
26	51.39	1.25	27.89	1.84	3.06	0.00	19.694	-19.69	0.00000	0	13.662	0.458	11.54	4.546	6.390
27	51.39	1.25	28.91	1.86	3.06	0.00	17.969	-17.97	0.00000	0	12.882	0.474	10.82	4.335	6.228
28	51.39	1.25	29.64	1.88	3.06	0.00	17.318	-17.32	0.00000	0	4.896	0.187	4.10	1.654	2.421
29	51.39	1.25	29.96	1.89	3.06	0.00	17.701	-17.70	0.00528	0.514	2.697	0.101	2.26	0.908	1.373
30	51.39	1.25	30.71	1.90	3.06	0.00	18.523	-18.52	0.00000	0	15.845	0.566	13.31	5.286	8.093
31	51.39	1.25	32.00	1.93	3.06	0.00	19.82	-19.82	0.00000	0	16.961	0.566	14.30	5.601	8.987
32	51.39	1.25	32.73	1.94	3.06	0.00	20.503	-20.50	0.00047	0	2.441	0.079	2.06	0.802	1.320
33	51.39	1.25	33.32	1.96	3.06	0.00	20.973	-20.97	0.00000	0	13.642	0.430	11.54	4.473	7.494
34	51.39	1.25	34.33	1.98	3.06	0.00	21.71	-21.71	0.00000	0	14.451	0.440	12.25	4.722	8.150
35	51.39	1.25	35.16	1.99	3.06	0.00	21.7	-21.70	0.00000	0	8.722	0.266	7.39	2.854	5.023
36	51.39	1.25	35.59	2.00	3.06	0.00	21.212	-21.21	0.00452	0.514	3.047	0.095	2.58	1.001	1.802
37	51.39	1.25	36.25	2.01	3.06	0.00	20.405	-20.41	0.00000	0	14.081	0.456	11.91	4.651	8.326
38	51.39	1.25	37.36	2.03	3.06	0.00	18.988	-18.99	0.00000	0	13.103	0.456	11.04	4.378	7.950
39	51.39	1.25	38.47	2.05	3.06	0.00	17.433	-17.43	0.00000	0	12.030	0.456	10.09	4.076	7.485
40	51.39	1.25	39.10	2.06	3.06	0.00	16.529	-16.53	0.00025	0	1.226	0.049	1.02	0.420	0.773
41	51.39	1.25	40.02	2.08	3.06	0.00	15.084	-15.08	0.00000	0	15.445	0.677	12.83	5.362	9.931
42	51.39	1.25	41.51	2.10	3.06	0.00	12.631	-12.63	0.00000	0	9.443	0.494	7.73	3.382	6.258
43	51.39	1.25	42.33	2.11	3.06	0.00	11.2	-11.20	0.00689	0.514	2.396	0.141	1.94	0.879	1.663
44	51.39	1.25	43.09	2.12	3.256	0.00	9.8094	-9.81	0.00000	0	6.357	0.428	5.02	2.419	4.342
45	51.39	1.25	44.23	2.14	3.256	0.00	7.6129	-7.61	0.00000	0	4.933	0.428	3.73	1.987	3.441
46	51.39	1.25	45.30	2.15	3.457	0.00	5.4616	-5.46	0.00000	0	2.948	0.357	2.02	1.320	2.096
47	51.39	1.25	45.82	2.16	3.457	0.00	4.3878	-4.39	0.00012	0	0.138	0.021	0.09	0.066	0.099
48	51.39	1.25	46.83	2.17	3.457	0.00	2.1635	-2.16	0.00000	0	2.276	0.695	0.76	1.476	1.660
													Σ	142.153	187.491

Table 8. Recapitulation of the hydro-mechanical role of vegetation on slope stability in trees and shrubs

Vegetation	*Location*	*Characteristics*		*Mechanical paramter*			*Hydrological parameter*	*FOS Increase*	*Source*
		DBH	***Height***	C_R	S_w	F_{wind}	u_a-u_w χ		
		(cm)	**(m)**	**(kPa)**	**(kPa)**	**(kN)**	***PWP Depth* (cm)**	**(%)**	
Trees									
Tectona grandis	Indonesia	7.64–22.29	6.5–11.5	0.398	0.307	1.215	[c.3]	-0.1–20.2 [c.4]	This study
Young Maesopsis eminii		4.14–11.15	3–5.5	0.191	0.057	0.514	[c.3]	5–22.3 [c.4]	
Old Maesopsis eminii		8.92–18.79	6.5–12.5	0.087	0.343	2.74	[c.3]	-2.2–36.2 [c.4]	
Maple	Iran	30.5	23.17	0.6–15	0.6 and 1.2	[a]	[a]	0.1–10.5	[12] [b.1]
Common ash		15.28	17.57	0.6–4	0.6 and 1.2	[a]	[a]	2.5–22	
Oriental Beech		[a]	1	[a]	[a]	[a]	[a]	[a]	
Persian Ironwood		[a]	13.31	[a]	[a]	[a]	[a]	[a]	
Alder		33	20.94	[a]	[a]	[a]	[a]	[a]	
Young Forest	Canada	[a]	[a]	0.25–3	0.6[b.2]	[a]	[a]	0–17.5	[33]
Mature Forest		[a]	[a]	0.25–5	0.6[b.2]	[a]	[a]	0–20	
Cedar	Alaska	[a]	[a]	3.9–5.9	5.2[b.3]	1 (in kPa)	[c.1]	[c.2]	[60]
Hemlock		[a]	[a]	3.9–5.9	5.2[b.3]	1 (in kPa)	[c.1]	[c.2]	
Spruce		[a]	[a]	3.9–5.9	5.2[b.3]	1 (in kPa)	[c.1]	[c.2]	
Cut four years ago.		[a]	[a]	3.9–5.9	5.2[b.3]	1 (in kPa)	[c.1]	[c.2]	
Cut two years ago		[a]	[a]	3.9–5.9	5.2[b.3]	1 (in kPa)	[c.1]	[c.2]	
Shrubs									
Chromolaena odorata	Indonesia	2.4–2.7	2 [b.1]	0.202	0.016	0	[c.3]	2.9–17.8 [c.4]	This study
Grass	Canada	[a]	[a]	1	0.6[b.2]	[a]	[a]	0–7.5	[33]
Shrubs		[a]	[a]	0.25–2	0.6[b.2]	[a]	[a]	0–15	

Note:
[a] : unknown or not specified.
[b] : [1]modified from another research; [2]assumed; [3]estimated
[c] : [1]measured by piezometric levels from 1965–1974; [2]The computed *FOS* are 1.1 or lower, the *FOS* of forest slope is greater than 1; [3]measured by Electrical Resistivity Tomography (ERT) method and modeled per 1 m depth; [4]modelled based on vegetation, PWP, and mechanical parameter scenario.

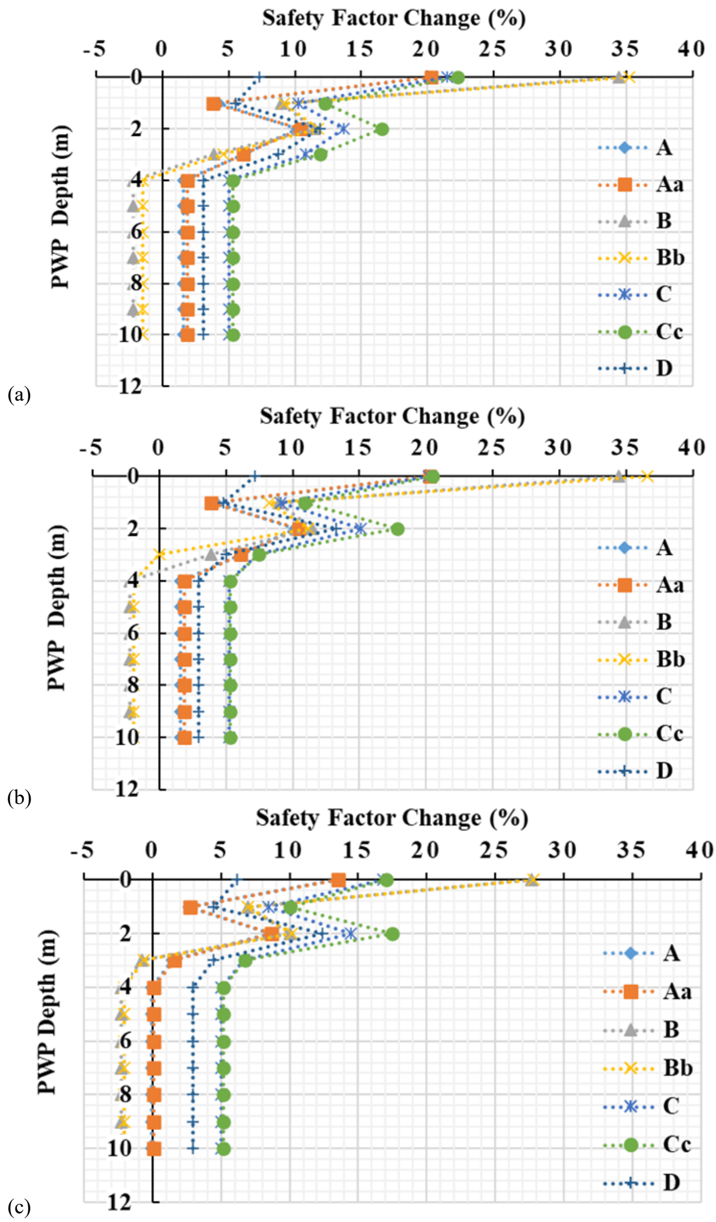

Fig. 8. FOS changes of bareland and slopes with vegetation based on soil mechanical parameters: (a) minimum, (b) average, (c) maximum

The significant FOS increase is in the PWP at the ground surface. FOS increases are <20.2% (scenarios A and Aa), <36.6% (scenarios B and Bb), <22.3% (scenarios C and Cc), and <7.3% (scenario D). Meanwhile, at a PWP depth of 1 m (scenario b), FOS decreased 2-6 times from before, then increased again at a PWP depth of 2 m, then reduced at a PWP depth of 3m (scenario d), and then stabilized in FOS at a PWP depth of >4m (Figure 9).

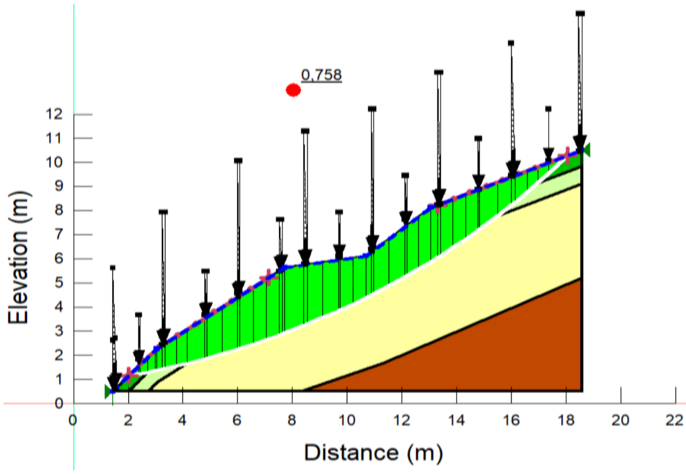

Fig. 9. Visualization of slope stability modeling in the Bb scenario, PWP = 0 and average soil mechanics parameters

Hand Calculation of Slope Stability Modeling

Hand calculations of slope stability scenarios, namely the young Maesopsis eminii + shrubs (Bb Simulation) with the phreatic line (PW=0m) and average soil mechanical parameters. Slope stability modeling using Geostudio-Slope/W is presented in Figure 9.

Seven slices of soil are used in the analysis, and parameters are obtained based on free body diagram information, which describes the forces acting on each slice, as shown in Figure 6. The hand calculation of the FOS is presented in Table 7 using trial and error. FOS is 0.614, and a final FOS of 0.758 was obtained. So, the FOS value from the modeling is the same as the result of the hand calculations.

The presence of vegetation can increase FOS compared to slopes without vegetation (bareland). The modeling explained an increase in FOS in every simulation except for the old Maesopsis eminii vegetation at a PWP depth of 3-4m. Old Maesopsis eminii has the largest mechanical parameters that decrease slope stability, namely vegetation surcharges (Sw) and wind load force (Fwind) compared to other vegetation, and also has the lowest root cohesion (CR) that can increase slope stability. The mechanical vegetation role (Sw and Fwind) as a shear stress function tends to be detrimental to slope stability. Fwind can increase slope stability if the slope steepness is smaller than the internal friction angle and vice versa [17, 51].

Modeling slope stability due to rainfall is important to consider PWP. Soil moisture increases during rain events, and then PWP varies temporally and spatially based on rainfall, soil, slope geometry, changes in soil physical, mechanical, and hydraulic properties, and land use [52]. Rainfall (pattern, distribution, intensity), especially during extreme rainfall events, is potentially destabilizing and causes slope failure. Slope failure is also influenced by initial soil moisture conditions [50].

Both hydrological and mechanical roles can increase or decrease slope stability. Soil moisture conditions, rainfall characteristics, interception, and vegetation characteristics influence the hydrological role. The mechanical role is affected by potential slip surface depth, the number, diameter, root tensile, and bending strength that cross the soil slip surface.

Root tensile strength rises as root diameter decreases, and large numbers of fine roots improve soil more efficiently than small amounts of coarse roots [53]. Field research on forested slopes that have root diameters of under 20mm contributes most to slope strengthening [54]. This study models root cohesion (CR) at root diameters under 10mm, which act as tensile fibers during slope failure and contribute to slope stability. In contrast, roots with a diameter of more than 10mm act as anchors rather than tensile fibers due to their stiffness [55].

The question regarding the effectiveness of fine versus coarse roots as slope reinforcement has a practical parallel in selecting trees versus shrubs. Shrubs have a higher CR and can be applied to increase slope stability since they have fine, shallow, and dense roots [56]. Sw and Fwind of shrubs on the slope are very small and tend to be neglected. Meanwhile, trees have properties that are inversely proportional to shrubs, except for young trees.

In dry conditions, trees have a higher hydrological role than shrubs, whereas, in wet situations, shrubs play a greater mechanical role [57, 58, 67]. Coniferous trees have higher slope stability in the winter than other kinds of trees and shrubs [59]. Vegetation type influences slope stability in various ways, influenced by tree geometry (trunk diameter, canopy type, and root depth) and the modulus of elasticity of trees and soil [37, 65].

Previous research states that the vegetation role on slopes can be influenced by several factors, namely slope steepness [17], root system (number, diameter, depth, morphology, tensile strength, and root area ratio) [6, 66], soil aggregate stability [34], season or weather (wet, dry, snow) [11, 60], vegetation type (diameter, height, canopy characteristics, shape, and bark) [37, 57, 61, 64], slope shape, vegetation location [62], plant spacing [63], and growing conditions [4].

The results of slope stability modeling based on eight slope cover scenarios with and without vegetation, 11 PWP scenarios, and 3 soil mechanical parameter scenarios show that the hydro-mechanical role of vegetation can influence slope stability. This research aligns with research carried out regarding slope stability modeling, which considers the hydro-mechanical parameters of vegetation, as presented in Table 8. Trees can generally increase FOS to a greater extent than shrubs, reaching an increase in FOS of 22% in Common ash [3]. This research shows that an increase in FOS can be 36% in old Maesopsis eminii. Meanwhile, shrubs can increase FOS by up to 15% [17], while this research shows an increase in FOS for shrubs, reaching 17% (Table 8).

Recent research related to other case studies helps verify and validate the methods, analysis results, and modeling that have been carried out. This last point is very important because modeling the role of hydromechanics, in this case, is the parameters of soil water content, matrix suction, root cohesion, vegetation load, and wind load forces in slope stability analysis depending on soil, geological, climatological, and vegetation characteristics. From the research location, the modeling and analysis results are very location-specific.

Conclusions

The hydrological role in the form of soil water content (χ) and matrix suction (u_a–u_w) (negative PWP) in unsaturated soil conditions is modeled based on the PWP depth every 1m. The mechanical roles of root cohesion (C_R), vegetation surcharges (S_w) and wind load force (F_{wind}) are each modeled by adding C_R and effective soil cohesion (c') to the soil mechanics parameters, S_w as a uniform load on the ground (surface surcharge), and F_{wind} as a point load on the ground surface. The modeling results show that the largest total C_R is for teak at 0.398kPa, followed by shrubs and young and old *Maesopsis eminii*, with total C_R values of 0.202, 0.191 and 0.087kPa, respectively. The larger the total C_R, the greater the root's contribution to increasing the soil shear strength. The S_w value in teak ranges from 0.121 to 0.121–0.307kPa, in young *Maesopsis eminii* ranges from 0.007–0.057kPa, in old *Maesopsis eminii* ranges from 0.022–0.343kPa, and the S_w value in shrubs is 0.016kPa. The maximum lateral wind load force in the teak and young and old *Maesopsis eminii* is 1,215.53 N, 514.68 N and 2,736.78 N.

The modeling results are then used as input to model the hydro-mechanical role of vegetation on slope stability using the modified SBM. The results of slope stability modeling show variations in *FOS* values in response to variations in the position of positive pore water pressure (PWP+). Old *Maesopsis eminii* slopes have the greatest increase in *FOS* values when PWP+ is at the ground surface, while when PWP+ is at a depth of >1.0m, the largest *FOS* value is young *Maesopsis eminii,* followed by shrub, teak, old *Maesopsis eminii*, and bareland. Modeling results on eight scenarios in teak, old *Maesopsis eminii*, young *Maesopsis eminii*, and shrubs show an increase in *FOS* values, namely 20.2%, 36.6%, 22.3%, and 7.3%, respectively. In general, the *FOS* value increases with the shallower phreatic line (PWP+) and the *FOS* value reaches stability (*FOS* >1) in PWP+ conditions at a depth of ≥4m, except in old *Maesopsis eminii,* where soil mechanical parameters are minimum. Vegetation in the form of old *Maesopsis eminii* reduces *FOS* by up to 2% when PWP+ ≥4 m because it has the largest S_w and F_{wind} and also has the smallest C_R among other vegetation. This research shows that the hydromechanical role of vegetation can increase slope stability compared to slopes without vegetation.

This research is helpful in Forest Management in understanding the dynamic and interactive process of a landslide event on a vegetated slope, material for consideration in landslide mitigation policies with vegetation, land management planning, and increasing community insight regarding landslide disasters. The hydro-mechanical vegetation on slope stability model provides a new approach to modeling natural landslides that improves understanding of scientific concepts related to forest management science in hydro-meteorological disasters, especially landslides based on the science of forest hydrology, mechanics, physics and soil hydraulics, and soil and water conservation.

Acknowledgments

The authors are grateful to the Program of Master leading to PhD (PMDSU) of the Ministry of Education, Culture, Research, and Technology of the Republic of Indonesia for supporting this study. We also thank all the landslide team who helped to collect data, do fieldwork, and do laboratory activity.

References

[1] * * *, BNPB (National Disaster Management Agency), **National Disaster Data**, 2024. http://dibi.bnpb.go.id/ (*in Indonesian*).

[2] V. Lupiano, V. Rago, O.G. Terranova, G. Iovine, *Landslide inventory and main geomorphological features affecting slope stability in the Picentino river basin (Campania, southern Italy)*, **Journal of Maps**, **15**, 2019, pp. 131-141. DOI: 10.1080/17445647.2018.1563836.

[3] M. Emadi-Tafti, B. Ataie-Ashtiani, S.M. Hosseini. *Integrated impacts of vegetation and soil type on slope stability: A case study of Kheyrud Forest, Iran*, **Ecological Modelling**, **446**, 2021, Article Number: 109498. DOI: 10.1016/j.ecolmodel.2021.109498.

[4] Y.A. Fata, Hendrayanto, Erizal, S.D. Tarigan, C. Wibowo, *Vetiver root cohesion at different growth sites in Bogor, Indonesia*, **Biodiversitas**, **23**, 2022, pp. 1683-1692. DOI: 10.13057/biodiv/d230360.

[5] R. Xu, W.L. Yang, C. Jiang, M. Rabiei, *Use of local plants for ecological restoration and slope stability: a possible application in Yan'an, Loess Plateau, China, Geomatics*, **Natural Hazards and Risk**, **10**, 2019, pp. 2106-2128. DOI: 10.1080/19475705.2019.1679891.

[6] Y.A. Fata, Hendrayanto, Erizal, S.D. Tarigan, T. Katsumi, *Modelling of mechanical roots on slope stability*, **Journal of Degraded and Mining Lands Management**, **10**, 2023, pp. 4779-4790. Doi: 10.15243/jdmlm.2023.104.4779.

[7] H. Zhu, L. Zhang, *Root-soil-water hydrological interaction and its impact on slope stability*, **Georisk: Assessment and Management of Risk for Engineered Systems and Geohazards**, **13**, 2019, pp. 349-38. DOI: 10.1080/17499518.2019.1616098.

[8] S. Bordoloi, C.W.W Ng, *The effects of vegetation traits and their stability functions in bioengineered slopes: A perspective review*, **Engineering Geology**, **275**, 2020, Article Number: 105742. DOI: 10.1016/j.enggeo.2020.105742.

[9] Y.A. Fata, Hendrayanto, Erizal, S.D. Tarigan, *2D and 3D ground model development for mountainous landslide investigation*, **IOP Conference Series: Earth and Environmental Science**, **871**, 2021, Article Number: 012057. DOI: 10.1088/1755-1315/871/1/012057.

[10] S. Feng, H.W. Liu, C.W.W. Ng, *Analytical analysis of the mechanical and hydrological effects of vegetation on shallow slope stability*, **Computers and Geotechnics**, 2020, Article number: 103335. DOI: 10.1016/j.compgeo.2019.103335.

[11] A. Gonzalez-Ollauri, S.B. Mickovski, *Hydrological effect of vegetation against rainfall-induced landslides*, **Journal of Hydrology**, **549**, 2017, pp. 374-387. DOI: 10.1016/j.jhydrol.2017.04.014.

[12] D.R. Greenway, M.G. Anderson, K.C. Brian-Boys (eds.), *Vegetation and slope stability*, **Slope Stability** Wiley: Chichester, 1987, pp. 187-230.

[13] R.C. Tiwari, N.P. Bhandary, R. Yatabe, D.R. Bhat, 2013, *Evaluation of factor of safety for vegetated and barren soil slopes with limit equilibrium computations*, **Geomechanics and Geoengineering**, **8**, 2013, 254-273. DOI: 10.1080/17486025.2012.744101.

[14] * * *, Geo-Slope International Ltd, **SLOPE/W for Slope Stability Analysis**, Calgary, Kadar air titik jenuh serat beberapa jenis kayu perdagangan Indonesia Alberta: Canada T2P 2Y5, 2002.

[15] B.R. Vinod, P. Shivananda, R. Swathivarma, M.B. Bhaskar, *Some of limit equilibrium method and finite element method based software are used in slope stability analysis*, **International Journal of Application or Innovation in Engineering Land & Management**, **6**, 2017, pp. 6-10.

[16] J.J. Ni, A.K. Leung, C.W.W. Ng, W. Shao, *Modelling hydro-mechanical reinforcements of plants to slope stability*, **Computers and Geotechnics**, **95**, 2018, pp. 99-109.DOI: 10.1016/j.compgeo.2017.09.001.

[17] N.K. Kokutse, A.G.T. Temgoua, Z. Kavazovic. *Slope stability and vegetation: Conceptual and numerical investigation of mechanical effects*, **Ecological Engineering**, **86**, 2016, pp. 146-153. DOI: 10.1016/j.ecoleng.2015.11.005.

[18] A. Mulyono, A. Subardja, I. Ekasari, M. Lailati, R. Sudirja, W. Ningrum, *The hydromechanics of vegetation for slope stabilization*, **IOP Conf. Series: Earth and Environmental Science, Global Colloquium on GeoSciences and Engineering 201718–19 October 2017, Bandung, Indonesia**, **118**, 2018, Article Number: 012038. DOI: 10.1088/1755-1315/118/1/012038.

[19] * * *, Climate-data.org, **Climate: Indonesia**, 2021. https://en.climate-data.org/asia/indonesia-101/.

[20] * * *, BPS (Statistics Indonesia), **Sukajaya District in numbers**, 2020. BPS Bogor Regency, (*in Indonesian*).

[21] * * *, ESDM (Ministry of Energy and Mineral Resources), **Ground movement inspection report in Sukajaya District, Bogor Regency, West Java**, 2020. vsi.esdm.go.id, (*in Indonesian*).

[22] * * *, Soil Survey Staff, **Key of Soil Taxonomy**, Third edition, BBSDLP, Bogor (ID), 2014, (*in Indonesian*).

[23] * * *, BBSDLP (Center for Research and Development of Agricultural Land Resources), ***Kunci Taksonomi Tanah*** **(Key of Soil Taxonomy)**, BBSDLP, Bogor (ID), 2016,

[24] * * *, SNI 3420, ***Metode uji kuat geser langsung tanah tidak terkonsolidasi dan tidak terdrainase*** **(Direct Shear Strength Test Method for Unconsolidated and Undrained Soil)**, *Badan Standarisasi Nasional* (National Standardization Agency), 2016.

[25] * * *, ASTM D3080-04, **Standard test method for direct shear test of soils under consolidated drained conditions**. ASTM International, 2012.

[26] * * *, ASTM D638-14, **Standard Test Method for Tensile Properties of Plastics**. United States, 2015.
[27] D.H. Gray, R.B. Sotir, **Biotechnical Soil Bioengineering Slope Stabilization: A Practical Guide for Erosion Control**, John Wiley & Sons, New York, 1996.
[28] T.H. Wu, W.P. McKinnell III, D.N. Swanston DN, *Strength of tree roots and landslides on Prince of Wales Island, Alaska*, **Canadian Geotechnical Journal**, **16**, 1979, pp. 19-33. DOI: 10.1139/t79-003.
[29] W. Ounban, L. Puangchit, S. Diloksumpun, *Development of general biomass allometric equations for Tectona grandis Linn.f. and Eucalyptus camaldulensis Dehnh. plantations in Thailand*, **Agriculture and Natural Resources**, **50**(1), 2016, pp. 48-53. DOI: 10.1016/j.anres.2015.08.001
[30] I. Samsoedin, H. Sukiman, M. Wardani, N.M. Heriyanto, *Pendugaan biomassa dan kandungan karbon kayu afrika (Maesopsis eminii Engl.) di Kabupaten Sukabumi, Jawa Barat (Estimation of biomass and carbon content of Maesopsis emenii Engl in Sukabumi Regency, West Java)*, **Jurnal Penelitian Hutan Tanaman**, **13**, 2016, pp. 73-81.
[31] A. Wibowo, H. Praptoyo, *Sifat fisika kayu jati pada kedudukan aksial dan radial (Physical properties of teak wood in axial and radial positions)*, **PhD Thesis**, Universitas Gadjah Mada, Yogyakarta (ID), 2013.
[32] A.R. Harijadi, *Kadar air titik jenuh serat beberapa jenis kayu perdagangan Indonesia (Water content of fiber saturation point of several types of Indonesian trade wood)*, **Bachelor Thesis**, Institut Pertanian Bogor, Bogor, 2009.
[33] S. Tjitrosoedirdjo, S.S. Tjitrosoedirdjo, R.C. Umaly, *The status of Chromolaena Odorata (L.) R.M. King and H. Robinson in Indonesia*, **Proceedings of the Second International Workshop on Biological Control of *Chromolaena Odorata***, 1991.
[34] M. Frei, *Validation of a new approach to determine vegetation effects on superficial soil movements*, **Doctoral Thesis**, Pfaffnau (LU): ETH Zurich, 2009.
[35] D.H. Gray, **Literature Review Greenbelt Consulting**, 2009, pp.1-23.
[36] A. Simon, A.J.C. Collison, *Quantifying the mechanical and hydrologic effects of riparian vegetation on streambank stability*, **Earth Surface Processes and Landforms**, **27**, 2002, pp. 527-546. DOI:10.1002/esp.325.
[37] Y. Kim, H. Rahardjo, L.D.T. Tieng, *Stability analysis of laterally loaded trees based on tree-root-soil interaction*, **Urban Forestry & Urban Greening**, 2020, Article Number: 126639. DOI: 10.1016/j.ufug.2020.126639.
[38] T.G. Sanz, A. Sanz-Andres, F.M. Canadas, G.M.A. Ortiz, *Wind Effect on Populus Sp*, **International Conference "Wind Effects on Trees**, 2003, pp. 1-7.
[39] L. Manickathan, T. Defraeye, J. Allegrini, D. Derome, J. Carmeliet, *Comparative study of flow field and drag coefficient of model and small natural trees in a wind tunnel*, **Urban Forestry & Urban Greening**, **35**, 2018, pp. 230-239. DOI: 10.1016/j.ufug.2018.09.011.
[40] E. de Langre. *Effects of wind on plants*, **Annual Review of Fluid Mechanics**, **40**, 2008, pp. 141-168. DOI: 10.1146/annurev.fluid.40.111406.102135.
[41] * * *, Geo-Slope International Ltd, **Stability Modeling with Geostudio**, Calgary, Alberta: Canada T2P 2Y5, 2021.
[42] B. Shen, J. Shi, N. Barton, *An approximate nonlinear modified Mohr-Coulomb shear strength criterion with critical state for intact rocks*, **Journal of Rock Mechanics and Geotechnical Engineering**, **10**, 2018, pp. 645-652. DOI: 10.1016/j.jrmge.2018.04.002.
[43] Y.H. Chok, W.S. Kaggwa, M.B. Jaksa, D.V. Griffiths, *Modelling the effects of vegetation on stability of slopes*, **9th Australia New Zealand Conference on Geomechanics**, Auckland (AU), 2004, pp. 391-397.
[44] C. O'Loughlin, R.R. Ziemer, *The importance of root strength and deterioration rates upon edaphic stability in steepland forests*, **Proceedings of I.U.F.R.O**, Workshop P.1.07-00 Ecology of Subalpine Ecosystems as a Key to Management, 1982.

[45] L. Wu, R. Huang, X.Li, **Hydro-mechanical analysis of rainfall-induced landslides**, Beijing: Springer Science Press, 2020. DOI: 10.1007/s12665-020-8878-8.

[46] R.H. Brooks, A.T. Corey, **Hydraulic Properties of Porous Media**, Hydrology Papers, Colorado State University, 1964.

[47] * * *, Geo-Slope International Ltd, **Seepage Modeling with SEEP/W**, Calgary, Alberta: Canada T2P 2Y5, 2015.

[48] G.T. Liong, D.J.G. Herman, ***Analisa stabilitas lereng limit equilibrium vs finite element method*** **(Slope stability analysis limit equilibrium vs finite element method)**, PIT HATHI XVI, Jakarta, 2012.

[49] A. Ibrahim, M. Mukhlisin, O. Jaafar, *Numerical assessment of rainfall infiltration into soil column for the unsaturated layered residual forest soil*, **Jurnal Teknologi**, **65**, 2013, pp. 121-127.

[50] L. Baninajarian, *Effect of future extreme precipitation events on the stability of soil embankments Across Ontario*, **PhD Thesis**, York University, Toronto, Ontario, 2020.

[51] E.B. Masi, S. Segoni, V. Tofani, *Root reinforcement in slope stability models: A Review*, **Geosciences**, **11**, 2021, Article Number: 212. DOI:10.3390/geosciences11050212.

[52] S. Beegum, P.J. Jainet, D. Emil, K.P. Sudheer, S. Das, *Integrated simulation modeling approach for investigating pore water pressure induced landslides*, **Research Square**, 2022, pp. 1-28. DOI: 10.21203/rs.3.rs-1186263/v1.

[53] B. Reubens, J. Poesen, F. Danjon, G. Geudens, B. Muys, *The role of fine and coarse roots in shallow slope stability and soil erosion control with a focus on root system architecture: a review*, **Trees**, **21**, 2007, pp. 385-402. DOI: 10.1007/s00468-007-0132-4.

[54] M.E. Styczen, R.P.C. Morgan**,** *Engineering properties of vegetation***. Morgan RPC. Rickson RJ (eds) Slope Stabilization and Erosion Control: A Bioengineering Approach**, London: E&FN Spon, 1995.

[55] M. Tosi, *Root tensile strength relationships and their slope stability implications of three shrub species in the Northern Apennines (Italy)*, **Geomorphology**, **87**, 2007, pp. 268-283. DOI: 10.1016/j.geomorph.2006.09.019.

[56] A. Kumar, S.K. Das, L. Nainegali, K.R. Reddy, *Investigation of root traits of Dendrocalamus strictus cultivated on organically amended coalmine overburden and its potential use for slope stabilization*, **International Journal of Phytoremediation**, **25**, 2023, pp. 1932-1944. DOI: 10.1080/15226514.2023.2208235.

[57] E. Arnone, D. Caracciolo, L.V. Noto, F. Preti, R.L. Bras, *Modeling the hydrological and mechanical effect of roots on shallow landslides*, **Water Resources Research, 52**(11), 2016, pp. 8590-8612. DOI: 10.1002/2015WR018227.

[58] F.T.Y. Leung, W.M. Yang, B.C.H. Hau, L.G. Tham, *Root systems of native shrubs and trees in Hong Kong and their effects on enhancing slope stability*, **Catena**, **125**, 2015, pp. 102-110. DOI: 10.1016/j.catena.2014.10.018.

[59] E. Hayati, E. Abdi, M.M. Saravi, J.L. Nieber, B. Majnounian, G.B. Chirico, B. Wilson, M. Nazarirad, *Soil water dynamics under different forest vegetation cover: Implications for hillslope stability*, **Earth Surface Processes and Landforms**, **43**(10), 2018, pp. 2106–2120. DOI: 10.1002/esp.4376.

[60] M. Bordoni, C. Meisina, R. Valentino, M.G. Persichilo, M. Bittelli, S. Chersich. *The impact of hydrological parameters on modelling slope safety factor towards shallow landslides: a case study from Oltrepò Pavese*, **E3S Web of Conferences**, 2016. DOI: 10.1051/e3sconf/20160915005.

[61] N. Osman, S.S. Barakbah, *Parameters to predict slope stability—Soil water and root profiles*, **Ecological Engineering**, **28**, 2006, pp. 90-95. DOI: 10.1016/j.ecoleng.2006.04.004.

[62] J. Ji, N. Kokutse, M. Genet, T. Fourcaud, Z. Zhang, *Effect of spatial variation of tree root characteristics on slope stability. A case study on Black Locust (Robinia pseudoacacia)*

and Arborvitae (Platycladus orientalis) stands on the Loess Plateau, China, **Catena**, **92**, 2012, pp. 139-154. DOI: 10.1016/j.catena.2011.12.008.

[63] A.G.T. Temgoua, N.K. Kokutse, Z. Kavazovic Z, *Influence of forest stands and root morphologies on hillslope stability*, **Ecological Engineering**, **95**, 2016, pp. 622-634. DOI: 10.1016/j.ecoleng.2016.06.073.

[64] Y.A. Fata, Hendrayanto, K. Murtilaksono, Erizal, *The role of hydro-mechanical vegetation in slope stability: A review*, **IOP Conference Series: Earth and Environmental Science**, **794**, 2021, Article Number: 012041. DOI: 10.1088/1755-1315/794/1/012041.

[65] H.C. Hardiyatmo, ***Tanah longsor dan erosi: kejadian dan penanganan*** **(Landslides and Erosion: Occurrence and Management)**, Yogyakarta (ID): UGM Pr, 2012.

[66] T.C.T. Hubble, D.W. Airey, H.K. Sealey, E.V.D. Carli, S.L. Clarke, 2013. *A little cohesion goes a long way: Estimating appropriate values of additional root cohesion for evaluating slope stability in the Eastern Australian highlands*, **Ecological Engineering**, **61**(C), 2013, pp. 621-632. DOI: 10.1016/j.ecoleng.2013.07.069.

[67] S.W. Rees, N. Ali, *Tree induced soil suction and slope stability*, **Geomechanics and Geoengineering**, 7, 2012, pp. 103-113. DOI: 10.1080/17486025.2011.631039.

Received: June 19, 2024
Accepted: March 20, 2025